Chapter 5
Modeling of the Energy and Matter Exchange

Within micrometeorology the term *modeling* is not uniquely defined. It refers to various methods covering a range of complexity extending from simple regressions up to complicated numerical models. In applied meteorology (agro meteorology and hydro meteorology) simple analytical models are very common. Modeling of evaporation is particularly important but sophisticated numerical methods are not yet widely used in this research area. The following chapter describes different types of models and their limitations beginning with simple analytical methods up to numerical models of near-surface energy and matter transport. The application of models in heterogeneous terrain receives special attention and related flux averaging approaches are addressed in a separate subchapter.

5.1 Energy Balance Methods

Energy exchange measurements and modeling form the bases for many applied investigations. Methods that are based on the surface energy balance equation (e.g. Bowen-ratio method, Sect. 4.2.2) are widespread regardless of the related open issues in terms of measurement techniques (see Sect. 3.8). Many applied models are based on similar theoretical backgrounds. Often, the general limitations of the various methods are unknown to the user. Most applications can be used only for hourly values at noon with unstable stratification or for daily and weekly averages (see below). Various models distinguish between potential evaporation from free water bodies or water saturated surfaces. The actual evapotranspiration, which is the sum of the evaporation of the soil and transpiration from plants, is typically lower.

In most of the models, parameters are used which were empirically determined by experiments. Strictly speaking, these parameters are only valid for the climatological conditions prevailing during the original experiments. The parameter values can vary from place to place, and more importantly they are valid only for special mean climatological conditions. Thus, the parameters are functions of the place, the time

T. Foken, *Micrometeorology*, DOI 10.1007/978-3-642-25440-6_5

of the year, and the weather or climate of the period when the experiment was done. These conditions may currently or in the future no longer be valid (Houghton 2015). Therefore, hourly and daily values have only a low representativeness. Depending on the sensitivity of the parameterization, decade or monthly averages have an acceptable accuracy. Accordingly, it is necessary to associate the time scale of the model with the intended use and the geographically valid region.

5.1.1 Determination of the Potential Evaporation

5.1.1.1 Dalton Approach

The simplest way to determine the potential evaporation over open water is the Dalton approach, which is comparable to the bulk approach discussed in Sect. 4.2.1 . It is not part of the energy balance methods. Instead of the Dalton number alone, simple correction functions are used which account for the wind-speed dependency,

$$\begin{aligned} Q_E &= f(u)\,[E(T_0) - e(z)], \\ f(u) &= a + b\,u^c, \end{aligned} \tag{5.1}$$

where a = 0.16; b = 0.2; c = 0.5 for lakes in Northern Germany (Richter 1977). Possible areas of application for this method are given in Table 5.1.

5.1.1.2 Turc Approach

Many approaches are based on radiation measurements, e.g. the evaporation calculation, where only the air temperature (t in °C) and the global radiation (in W m^{-2}) are used as input parameters (Turc 1961):

$$Q_{E\text{-}TURK} = k\,(K\downarrow + 209)\frac{0.0933t}{t+15} \tag{5.2}$$

Table 5.1 Possible areas of application of the Dalton approach

Criterion	Evaluation
Defining quantity	Potential evaporation of free water bodies
Area of application	According to the validity of the area specific constants (DVWK 1996)
Resolution of ten input parameters	10–60 min averages
Representativeness of the results	(daily-), decade and monthly averages
Error	20–40%

Table 5.2 Possible areas of application of the Turc approach

Criterion	Evaluation
Defining quantity	Potential evaporation of free water bodies, possible for well saturated meadows
Area of application	Mediterranean Sea, Germany (lowlands) with correction factor k = 1.1
Resolution of ten input parameters	10–60 min averages
Representativeness of the results	Decade and monthly averages
Error	20–40%

The method was developed for the Mediterranean Sea and for the application in Germany Eq. (5.2) needs a correction factor of about k = 1.1 (DVWK 1996). Possible areas of application for this method are given in Table 5.2.

5.1.1.3 Priestley–Taylor Approach

The Bowen ratio is the starting point for the derivation of several methods for the determination of sensible and latent heat fluxes. The Priestley–Taylor approach starts with Eqs. (2.98) and (4.7) respectively, which can be written with the potential temperature and the dry adiabatic temperature gradient as:

$$Bo = \gamma \frac{\partial \overline{\theta}/\partial z}{\partial \overline{q}/\partial z} = \frac{\gamma \left[\left(\partial \overline{T}/\partial z\right) + \Gamma_d\right]}{\partial \overline{q}/\partial z} \tag{5.3}$$

With the temperature dependence of saturation water vapor pressure according to the Clausius–Clapeyron's equation

$$\frac{d\,q_s}{dT} = s_c\left(\overline{T}\right) \tag{5.4}$$

it follows that

$$Bo = \frac{\gamma \left[\left(\partial \overline{T}/\partial z\right) + \Gamma_d\right]}{s_c \left(\partial \overline{T}/\partial z\right)} = \frac{\gamma}{s_c} + \frac{\gamma\, \Gamma_d}{s_c \left(\partial \overline{T}/\partial z\right)}, \tag{5.5}$$

where γ is the psychrometric constant in K^{-1}.

For the further derivation, the second term on the right-hand-side of (5.5) will be ignored; however, this is valid only if the gradient in the surface layer is significantly greater than the dry adiabatic gradient of $\Gamma_\mathrm{d} = 0.0098\ \mathrm{K\ m}^{-1}$. This is not the case for neutral stability, because under such conditions the fluxes are generally small. After introducing the Priestley–Taylor coefficient of $\alpha_{PT} \sim 1.25$ for water

Table 5.3 Values for the temperature dependent parameters γ und s_c based on the specific moisture (Stull 1988)

Temperature in K	γ in K^{-1}	s_c in K^{-1}
270	0.00040	0.00022
280	0.00040	0.00042
290	0.00040	0.00078
300	0.00041	0.00132

Table 5.4 Possible areas of application of the Priestley–Taylor approach

Criterion	Evaluation
Defining quantity	Potential evaporation of free water bodies
Area of application	Universally
Resolution of ten input parameters	10–60 min averages
Representativeness of the results	(daily-), decade and monthly averages
Error	10–20%

saturated surfaces and applying the energy balance equations (1.1) and (4.8) respectively, follows the Priestley–Taylor approach (Priestley and Taylor 1972):

$$Q_H = \frac{[(1-\alpha_{PT})\, s_c + \gamma]\left(-Q_s^* - Q_G\right)}{s_c + \gamma} \tag{5.6}$$

$$Q_E = \alpha_{PT}\, s_c \frac{-Q_s^* - Q_G}{s_c + \gamma} \tag{5.7}$$

Typical values of the ratios $c_p/\lambda = \gamma$ and $de_s/dT = s_c$ are given in Table 5.3 and can be calculated approximately with the following relation:

$$\frac{s_c}{\gamma} = -0.40 + 1.042\, e^{0.0443 \cdot t} \tag{5.8}$$

The method can be used for vegetated surfaces if the Priestley–Taylor coefficient is varied to account for the dependence on stomata resistance (DeBruin 1983). Possible areas of application for this method are given in Table 5.4.

5.1.1.4 Penman Approach

A commonly used method for the determination of the potential evaporation is that proposed by Penman (1948). This method was developed for Southern England and underestimates the evaporation for arid regions. The derivation is based on the Dalton approach and the Bowen ratio, whereas the equation of the Priestley–Taylor type is an intermediate stage (DVWK 1996). The evaporation in mm d^{-1} is

Table 5.5 Wind factors in the ventilation term of Eq. (5.10)

Surface and reference	f_1 in mm d^{-1} h Pa^{-1}	f_2 in mm d^{-1} h Pa^{-1} m^{-1} s
Original approach for water bodies (Hillel 1980)	0.131	0.141
Small water bodies (DVWK 1996)	0.136	0.105
Water bodies (Dommermuth and Trampf 1990)	0.0	0.182
Grass surfaces (Doorenbos and Pruitt 1977; Schrödter 1985)	0.27	0.233

$$Q_E\left[\text{mm d}^{-1}\right] = \frac{s_c\left(-Q_s^* - Q_G\right)\left[\text{mm d}^{-1}\right] + \gamma\, E_a\left[\text{mm d}^{-1}\right]}{s_c + \gamma}, \tag{5.9}$$

where the available energy must be used in mm d^{-1}. The conversion factor from mm d^{-1} to W m^{-2} is 0.0347. The second term in the numerator of Eq. (5.9) is called the ventilation term E_a (also in mm d^{-1}) and contains the influence of turbulence according to the Dalton approach. It is significantly smaller than the first term and is often ignored in the simplified Penman approach (Arya 2001). The Priestley–Taylor approach follows when α_{PT} = 1.0.

The ventilation term is a function of the wind velocity and the saturation deficit:

$$E_a = (E - e)\,(f_1 + f_2\, u)\,\left[\text{mm d}^{-1}\right] \tag{5.10}$$

While one can use daily averages in Eq. (5.10), the use of 10–60 min averages is considerably more meaningful; however, in this case the units must be converted. Typical values for both wind factors f_1 and f_2 are given in Table 5.5. These values are valid for water surfaces, but they can also be used for well-saturated grass surfaces, which to a large degree is the actual evaporation. To include the effects of larger roughness, the ventilation term according to the approach by van Bavel (1986) can be applied in h Pa ms^{-1}:

$$E_a = \frac{314\ \text{K}}{T}\,\frac{u}{\left[\ln(z/z_0)\right]^2}\,(E - e)\,\left[\text{h Pa m s}^{-1}\right] \tag{5.11}$$

Possible areas of application for this method are given in Table 5.6.

Table 5.6 Possible areas of application of the Penman approach

Criterion	Evaluation
Defining quantity	Potential evaporation of free water bodies
Area of application	Universally
Resolution of ten input parameters	10–60 min averages
Representativeness of the results	(daily-), decade and monthly averages
Error	10–20%

Table 5.7 Methods for the determination of the potential evaporation of water bodies. The underlying grey scale corresponds to the accuracies given in the last line

minute				
hour day decade month	Dalton approach	Turc approach	Priestley-Taylor approach	Penman approach
very good	good	satisfactory	rough estimate	inadequately
5–10 %	10–20 %	20–40 %	40–100 %	> 100 %

5.1.1.5 Overall Evaluation of Approaches for the Determination of the Potential Evaporation

All approaches presented thus far are valid only for computing longer-term averages. Less sophisticated approaches have only low accuracy for short averaging intervals (Table 5.7).

The inherent non-linearity of the approaches requires calculations using 30–60 min averages, but the results are not reliable for these short time periods.

5.1.2 Determination of the Actual Evaporation

Empirical methods for the determination of evaporation are widely used, but are only applicable in the specific areas for which they were developed. Therefore, these types of approaches were not included in the following chapter. However, methods developed by Haude (1955) and Sponagel (1980) or the modified Turc approach according to Wendling et al. (1991), which are commonly used in Germany, are described in detail in the German versions of this book (Foken 2016).

5.1.2.1 Penman–Monteith Approach

The transition from the Penman to the Penman–Monteith approach (Penman 1948; Monteith 1965; DeBruin and Holtslag 1982) included the consideration of non-saturated surfaces and cooling due to evaporation, which reduces the energy of

the sensible heat flux. Including both aspects leads to the Penman–Monteith method for the determination of the actual evaporation (evapotranspiration)

$$Q_H = \frac{\gamma\,\left(-Q_s^* - Q_G\right) - \rho c_p\, F_w}{R_G\, s_c + \gamma}, \tag{5.12}$$

$$Q_E = \frac{R_G\, s_c\left(-Q_s^* - Q_G\right) + \rho c_p\, F_w}{R_G\, s_c + \gamma}, \tag{5.13}$$

with the so-called ventilation term

$$F_w = C_E\, \overline{u}\, \left(R_G - R_s\right)\; q_{sat}, \tag{5.14}$$

where R_G is the relative humidity of the surface; R_s is the relative humidity close to the surface, and q_{sat} is the specific humidity for saturation. Eq. (5.14) can also be formulated according the resistance concept (see Sect. 5.3) without the molecular-turbulent resistance:

$$F_w = \frac{q_{sat} - q_a}{r_a + r_c} \tag{5.15}$$

In the simplest case, the canopy resistance, r_c, will be replaced by the stomatal resistance r_s. The stomatal resistance can be calculated from the stomatal resistance of a single leaf r_{si} and the leaf-area index (*LAI*, leaf surface of the upper side per area element of the underlying surface)

$$r_s = \frac{r_{si}}{LAI_{aktiv}}, \tag{5.16}$$

where LAI_{aktiv} is the leaf area index of the active sunlight leafs. Generally, this is only the upper part of the canopy, and therefore $LAI_{aktiv} = 0.5\ LAI$ (Allen et al. 1998). In the simplest case, the turbulent resistance is given (Stull 1988) as:

$$r_a = \frac{1}{C_E \overline{u}}. \tag{5.17}$$

But usually r_a is calculated from Eqs. (2.60) and (2.64):

$$r_a = \frac{\ln\left(\frac{z-d}{z_0}\right)\;\ln\left(\frac{z-d}{z_{oq}}\right)}{\kappa^2 u(z)} \tag{5.18}$$

In the non-neutral case, universal functions can be used in Eq. (5.18). Typical values of the parameters are given in Table 5.8. Possible areas of application for this method are given in Table 5.9.

Table 5.8 Typical values of the *LAI* (Kaimal and Finnigan 1994) and the stomata resistance of single leafs (Garratt 1992)

Surface	Height in m	*LAI* in $m^2\ m^{-2}$	r_{si} in $s\ m^{-1}$
Seat (begun to grow)	0.05	0.5	
Cereal	2	3.0	50–320
Forest	12–20	1–4	120–2700

Table 5.9 Possible areas of application of the Penman–Monteith approach

Criterion	Evaluation
Defining quantity	Actual evaporation
Area of application	Universally
Resolution of ten input parameters	10–60 min averages
Representativeness of the results	Hourly and daily averages
Error	10–40%

The Food and Agriculture Organization of the United Nations (FAO) has put much effort into the development of a uniform method to determine the evaporation, and recommended a more convenient equation with a limited input data set (Allen et al. 1998; Moene and van Dam 2014):

$$Q_E = \frac{s_c\left(-Q_s^* - Q_G\right) + \rho\, c_p \frac{0.622}{p} \frac{E-e}{r_a}}{s_c + \gamma\left(1 + \frac{r_s}{r_a}\right)}, \tag{5.19}$$

where r_s and r_a are given by Eqs. (5.16) and (5.18), respectively. The factor $0.622/p$ was included contrary to the original reference, and is necessary for consistency; the constants s_c and γ are used in the dimension K^{-1} and not as in the original reference, i.e. h Pa K^{-1}. Further improvements are still proposed like e.g. including the surface temperature such that parametrizations for the resistances are no longer needed (Mallick et al. 2015).

To compare worldwide evaporation rates and to use input parameters, which are available everywhere, the FAO has formulated a (grass) reference evaporation (Allen et al. 1998). This is based in principle on Eq. (5.19), but includes the estimated input parameters given in Table 5.10. A further standardization was made by ASCI (American Society of Civil Engineers) by the unification of the calculation steps and application to grass and alfalfa (Allen et al. 2005).

The Penman–Monteith approach is widely used in diverse applications, for example, in the atmospheric boundary conditions of many hydrological and ecological models. During the daytime, the accuracy of computed hourly data is satisfactory, and the determination of daily sums of the evaporation and sensible heat fluxes is generally acceptable.

Table 5.10 Fixing of the input parameters for the FAO-(grass)-reference evaporation (Allen et al. 1998)

Parameter	Value	Remark
r_a	$d = 2/3\ z_B$; $z_0 = 0.123\ z_B$; $z_{0q} = 0.1\ z_0$ with $z_B = 0.12$ m and $z = 2$ m follows $r_a = 208/u$ (2 m)	It is $\kappa = 0.41$ applied
r_s	$LAI_{aktiv} = 0.5\ LAI$; $LAI = 24\ z_B$ with $r_{si} = 100$ s m^{-1} and $z_B = 0.12$ m follows $r_s = 70$ s m^{-1}	
$-Q_s^* - Q_G$	Various simplifications possible with an albedo of 0.23	Allen et al. (1998)

The available energy is the main forcing, but because the atmospheric turbulence and the control by the plants influence the ventilation term, the method is inaccurate if the turbulent conditions differ from an average stage. Therefore, this approach is often not used in meteorological models that have several layers in the surface layer (see Sect. 5.3).

Other approaches not discussed here require long averaging intervals and thus have low accuracy for short averaging periods. Water balance methods use the water balance equation Eq. (1.23) while runoff and precipitation are measured parameters.

5.1.3 *Determination from Routine Weather Observations*

The equations presented up to here are generally not adequate to determine the energy exchange from routinely available observations. Holtslag and van Ulden (1983) developed a method to determine the sensible heat flux under application of the Priestley–Taylor approach. They included an advection factor $\beta = 20$ W m^{-2} according to DeBruin and Holtslag (1982), and varied α_{PT} with the soil moisture between 0.95 and 0.65; however, for summer conditions with good water supply $\alpha_{PT} = 1.0$ can be assumed. Eq. (5.6) then has the following form with temperature-dependent constants according to Table 5.3:

$$Q_H = \frac{[(1-\alpha_{PT})\ s_c + \gamma]\ \left(-Q_s^* - Q_G\right)}{s_c + \gamma} + \beta \tag{5.20}$$

To estimate the available energy an empirical equation is used

$$\left(-Q_s^* - Q_G\right) = 0.9\frac{(1-\alpha)K\downarrow + c_1 T^6 - \sigma T^4 + c_2 N}{1 + c_3}, \tag{5.21}$$

where T is the air temperature; N is the cloud cover; $K\downarrow$ is the downward radiation; α is the surface albedo, and the constants $c_1 = 5.3 \cdot 10^{-13}$ W m^{-2} K^{-6}, $c_2 = 60$ W m^{-2} and $c_3 = 0.12$. The disadvantage of this method is that the cloud cover

Table 5.11 Possible areas of application of the Holtslag-van-Ulden approach

Criterion	Evaluation
Defining quantity	Sensible heat flux and actual evaporation
Important input parameters	Cloud cover (original method) Global radiation (modified method)
Area of application	Universally
Resolution of ten input parameters	10–60 min averages
Representativeness of the results	Hourly and daily averages
Error	10–30%

from routine weather observations is often not available. The application is limited to daylight hours with either neutral or unstable stratification and neither rain nor fog.

Göckede and Foken (2001) have tried to only use, instead of the cloud cover, the widely-measured global radiation as input parameter. They applied a parameterization for the radiation fluxes based on cloud observations proposed by Burridge and Gadd (1977), see Stull (1988), to determine a general formulation for the transmission in the atmosphere, see Eqs. (1.5) and (1.7). The available energy is then given by

$$\left(-Q_s^* - Q_G\right) = 0.9 \text{ K} \downarrow \left(1 - \alpha - \frac{0.08 \text{ K m s}^{-1}}{K \downarrow_G}\right), \tag{5.22}$$

where $K\downarrow$ is the measured global radiation, and $K\downarrow_G$ is the global radiation near the surface which can be calculated from the extraterrestrial radiation and the angle of incidence:

$$K \downarrow_G = K \downarrow_{extr} (0.6 + 0.2 \sin \Psi) \tag{5.23}$$

With Eq. (5.25) it is only necessary to calculate the angle of incidence for hourly data using astronomical relations (Appendix A.4). The method can be applied to both Eq. (5.20) and the Penman–Monteith approach Eq. (5.12). As shown in Table 5.11, the areas of application of this method are similar to the ones of the method by Holtslag and van Ulden (1983). Both methods as well as the method by Burridge and Gadd (1977) give comparable results.

5.2 Hydrodynamical Multilayer Models

The development of multilayer models began soon after the start of hydrodynamic investigations (see Sect. 1.3). In these models, the energy exchange in the molecular boundary layer, the viscous buffer layer, and the turbulent layer of the surface layer (Fig. 1.4) was separately parameterized according to the particular exchange conditions. The exchange of sensible heat can be shown to be dependent on the

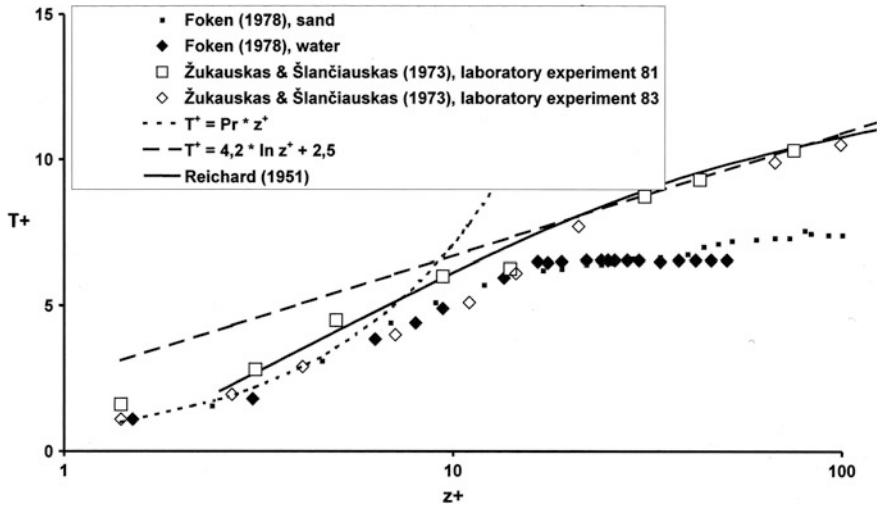

Fig. 5.1 Dimensionless temperature profile (T^+: dimensionless temperature, z^+: dimensionless height) according to laboratory measurements (Shukauskas and Schlantschiauskas 1973), and outdoor measurements (Foken 1978) and balanced profiles for the molecular layer (*dotted line*) and the turbulent layer (*broken line*) as well as profiles according to Reichardt (1951), from Foken (2002, with kind permission of © Borntraeger, Stuttagrt 2002, www.schweizerbart.de, All rights reserved)

temperature profile in dimensionless coordinates (Fig. 5.1) with the dimensionless height $z^+ = zu_*/\upsilon$ and the dimensionless temperature $T^+ = T/T_*$ (T_*: dynamical temperature) analogous to the wind profile with dimensionless velocity $u^+ = u/u_*$ (Landau and Lifschitz 1987; Csanady 2001; Schlichting and Gersten 2006). For the molecular boundary layer, $T^+ \sim z^+$, and for the laminar boundary layer $u^+ \sim z^+$. Above the viscous buffer layer, the flow is turbulent. Therefore, the typical logarithmic profile equations $T^+ \sim \ln z^+$ and $u^+ \sim \ln z^+$ are valid. The greatest problem for the parameterization is the formulation for the buffer layer, where empirical approaches must be applied. According to Fig. 5.1, profiles in the nature and in hydrodynamic studies (Foken 2002) are similar, which can be applied,

The hydrodynamic multilayer models based on bulk approaches, where instead of the bulk coefficients the so-called profile coefficient Γ is included, can be determined by integration over all layers

$$Q_H = -\Gamma[T(z) - T_0], \tag{5.24}$$

$$\Gamma = \left(\int_0^z \frac{dz}{K_T + v_{Tt} + v_T} \right)^{-1}, \tag{5.25}$$

where K_T is the turbulent diffusion coefficient for heat, v_{Tt} is the molecular-turbulent diffusion coefficient in the buffer layer, and v_T is the molecular diffusion coefficient.

The first integrations were done by Sverdrup (1937/38) and Montgomery (1940) using a single viscous sublayer consisting of the buffer layer and the molecular boundary layer. For this combined layer, a dimensionless height $\delta_{vT}{}^{+} \approx 27.5$ was assumed (this value is slightly larger than the values assumed today), and for the turbulent layer a logarithmic wind profile with roughness length z_0 was applied. For smooth surfaces an integration constant instead of the roughness length was used (von Kármán 1934).

An integral approach for all layers including the turbulent layer was presented by Reichard (1951), who parameterized the ratio of the diffusion coefficient and the kinematic viscosity

$$\frac{K_m}{\nu} = \kappa \left(z^{+} - z_T^{+} \tanh \frac{z^{+}}{z_T^{+}} \right). \tag{5.26}$$

This approach is in good agreement with experimental data as shown in Fig. 5.1, and can be used for the parameterization of exchange processes between the atmosphere and the surface (Kramm et al. 1996a) .

In the 1960s and 1970s, several papers were published with an integration of the profile coefficient over all three layers (Kitajgorodskij and Volkov 1965; Mangarella et al. 1972, 1973; Bjutner 1974). These models were based on new hydrodynamic data sets and took into account the wavy structure of the water surface (Foken et al. 1978) in the determination of the thickness of the molecular boundary layer

$$\delta_T = 7.5 \frac{\upsilon}{u_*} [\, 2 + \sin(\zeta - \pi/2) \,], \tag{5.27}$$

where $\varsigma = 0$ is valid for the windward and $\varsigma = \pi$ for the leeward site.

From measurements of the dimensionless temperature profile near the sea surface, it was possible to determine the dimensionless temperature difference in the buffer layer as $\delta_T{}^{+} \approx 4$ (Foken et al. 1978; Foken 1984); also compare with Fig. 5.1. Following this approach, by applying of Eq. (5.27) with $\varsigma = 0$ or $\delta_T \approx 6$ respectively for smooth surfaces and low friction velocities ($u_* < 0.23\,\mathrm{m\,s^{-1}}$) the profile coefficient is given by:

$$\Gamma = \frac{\kappa\, u_*}{\kappa\ \mathrm{Pr}\ \frac{\delta_T u_*}{\upsilon} + \kappa\, \delta_T^{+} + \ln \frac{u_* z}{30\, \nu}} \tag{5.28}$$

This model shows good results in comparison with experimental data (Foken 1984, 1986; Biermann et al. 2014), and can be used for the calculation of the surface temperature for known sensible heat flux (Lüers and Bareiss 2010). However, these approaches have not been widely used, which is primarily due to the fact that current models use fundamentally different approaches to describe the energy exchanges in the surface layer (Geernaert 1999), as it is further discussed in Sect. 5.5.

5.3 Resistance Approach

Recent models for the determination of the turbulent exchange are layer models. These models generally use the resistance approach for the energy and matter exchange between the atmosphere and the ground surface. They can be classified in three types:

One-layer-models consider only soil, plants and atmosphere at a close range. The plants are not separated into different layers. Instead, it is assumed that plants act like a big leaf covering the soil (*big leaf model*). Many of the so-called Soil-Vegetation-Atmosphere-Transfer (SVAT) models can be considered big-leaf models, but some SVAT models are multilayer models. These models are mainly based on surface layer physics (partly several layers) and are schematically illustrated in Fig. 5.2 (Hicks et al. 1987; Sellers and Dorman 1987; Schädler et al. 1990; Groß 1993; Kramm et al. 1996b; Gusev and Nasonova 2010). A special case is the hybrid model according to Baldocchi et al. (1987). One important requirement is the closure of the energy balance at the earth's surface. This can be reached with an iterative determination of the surface temperature (Mengelkamp et al. 1999), with is used in the parameterizations for both the energy fluxes and the longwave radiation.

Multilayer models simulate the atmosphere in several layers. The simplest models have no coupling with the atmospheric boundary layer, and only the surface layer is solved in detail. These models are available using simple (1st and 1.5th

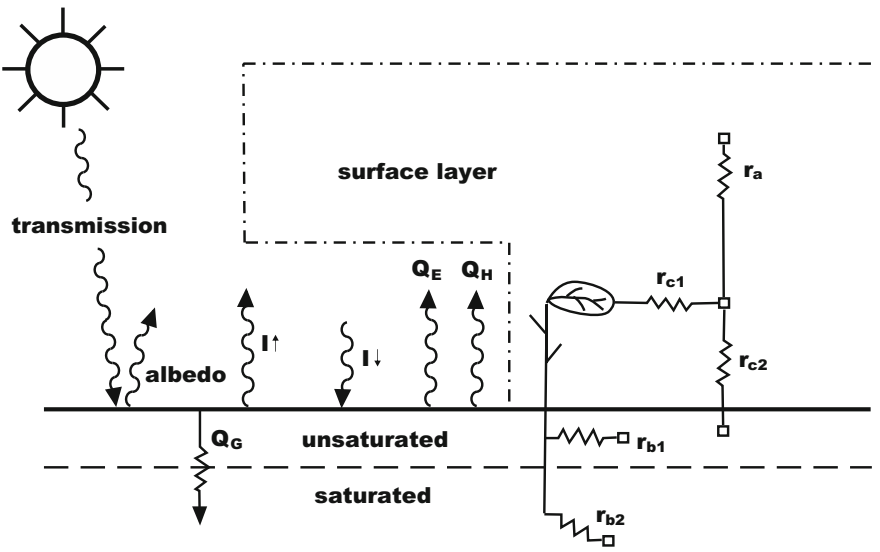

Fig. 5.2 Schematic representation of the modeling of the atmospheric surface layer including plants and soil (Blackadar 1997, adapted with kind permission of © Springer Berlin, Heidelberg 1997, All rights reserved)

order) and higher order closure techniques (Meyers and Paw U 1986, 1987; Baldocchi 1988; Pyles et al. 2000).

Multilayer models with boundary layer coupling best represent the current state of model development. In these models, the lower layers deal with balance equations, and the upper layers use assumptions based on mixing length approaches (Fig. 5.3, see Sect. 2.1.3). These models are also available with simple (1st and 1.5th order) and higher order closure techniques. The most widely used models use a 1st order closure with a local mixing length approach (Mix et al. 1994) or a non-local transilient approach (Inclán et al. 1996). The complicated transport conditions in high vegetation (see Sect. 3.5) may be best realized with a higher order closure technique (Pyles et al. 2000), which also accounts for the effects of coherent structures. An intercomparison showed that first order closure models do not adequately describe the fluxes at night (Staudt et al. 2011).

The resistance concept is based on the assumption that in the turbulent layer the turbulence resistance counteracts the turbulent flux, in the viscous and molecular layer a molecular-turbulence resistance counteracts the flux, and in the plant and soil all resistances can be combined into a total resistance (canopy resistance). The canopy resistance can be divided into different transfer pathways, where the main transport paths are stomata–mesophyll, cuticula, or direct transfer to the soil, which are schematically illustrated in Fig. 5.4. The simplest picture is the comparison with Ohm's law:

$$I = \frac{U}{R} \tag{5.29}$$

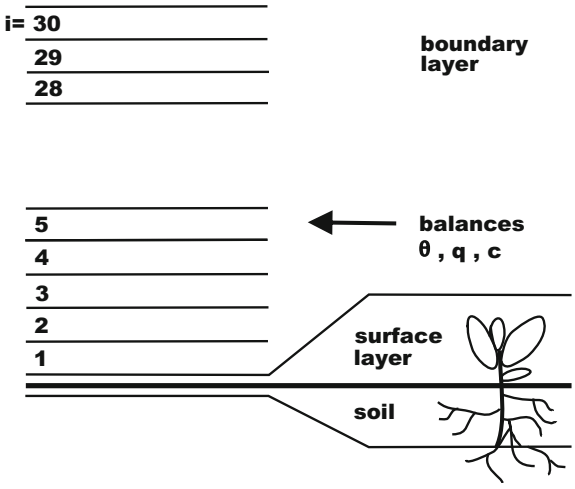

Fig. 5.3 Schematic representation of a boundary layer model (Blackadar 1997, adapted with kind permission of © Springer Berlin, Heidelberg 1997, All rights reserved)

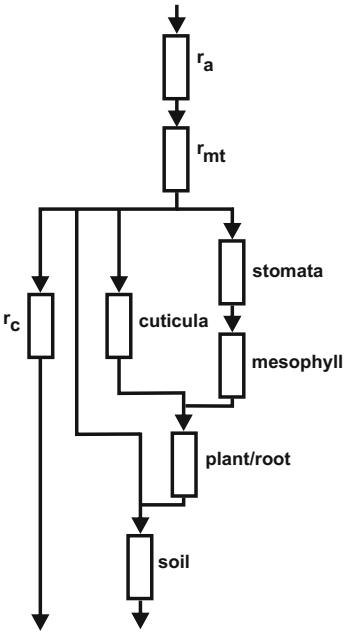

Fig. 5.4 Schematic representation of the resistance concept

Here, the flux is analogous with the current, I, and the vertical difference of wind speed or temperature with the voltage, U. The resistance, R, can be described as a network of individual resistances (Fig. 5.4) in the following simple form:

$$r_g = r_a + r_{mt} + r_c \tag{5.30}$$

The consideration of the resistance concept in the profile equations (Eqs. 2.48–2.50) is illustrated in the example of the sensible heat flux:

$$Q_H = -K(z)\frac{\partial T}{\partial z} = \frac{\int_{T(0)}^{T(z)} dT}{\int_0^z \frac{dz}{K(z)}} = \frac{T(z) - T(0)}{\int_0^z \frac{dz}{K(z)}} \tag{5.31}$$

For the bulk approaches (Eqs. 4.1–4.3) follows

$$Q_H = -C_H\, u(z)\,[T(z) - T(0)] = -\Gamma_H\,[T(z) - T(0)], \tag{5.32}$$

where the total resistance is:

$$r_{g(0,z)} = \int_0^z \frac{dz}{K(z)}, \tag{5.33}$$

$$r_{g(0,z)} = \frac{1}{\Gamma_{H(0,z)}} \tag{5.34}$$

The individual parts of the total resistance must be parameterized. For the turbulent resistance Eq. (2.86) under consideration of Eq. (2.67) is applied (Foken et al. 1995)

$$r_a = \int_{\delta}^{z_R} \frac{dz}{K(z)} = \frac{1}{\kappa u_*} \left[\ln \frac{z_R - d}{\delta - d} - \psi_H\left(\varsigma_{z_R}, \varsigma_\delta\right) \right], \tag{5.35}$$

where z_R is the reference level of the model, i.e. the upper layer of the model in the surface layer. The lower boundary, δ, is identical with the upper level of the molecular-turbulent layer. The resistance in the molecular-turbulent range is

$$r_{mt} = \int_{z_0}^{\delta} \frac{dz}{(D + K_H)} = (u_* B)^{-1}, \tag{5.36}$$

with the so-called sublayer-Stanton number B (Kramm et al. 1996a, 2002)

$$B^{-1} = Sc \int_0^{\eta} \frac{d\eta}{1 + ScK_m/v}, \tag{5.37}$$

$$\eta = u_*(z - z_0)/v, \tag{5.38}$$

and the Schmidt number in the case of the exchange of gases including water vapor

$$Sc = v/D. \tag{5.39}$$

For the exchange of sensible heat, the Schmidt number in Eq. (5.37) is replaced by the Prandtl number.

While parameterization with multilayer models (see Sect. 5.2) could be an obvious choice, presently most models use roughness length parameterizations (Jacobson 2005)

$$r_{mt} = \ln\left(\frac{z_0}{z_{0q}}\right) \frac{(Sc/\,\mathrm{Pr})^{2/3}}{\kappa\, u_*}, \tag{5.40}$$

with Pr = 0.71 and Sc = 0.60 valid in the temperature range of 0–40 °C. For the sensible heat flux follows for the sublayer -Stanton number according to Eqs. (5.36) and (5.40), (Owen and Thomson 1963):

$$\kappa\, B^{-1} = \ln \frac{z_0}{z_{0T}} \tag{5.41}$$

This equation is defined only for $z_0 > z_{0T}$, otherwise negative molecular-turbulent resistances would be calculated which are non-physical (Kramm et al. 1996a; Kramm et al. 2002). Nevertheless, in the literature negative values can be found (Brutsaert 1982; Garratt 1992), which can compensate for too large resistances in the turbulent layer and in the canopy, but in reality these negative values are due to inaccurate concepts of roughness lengths for scalars. For $\kappa\, B^{-1}$ values of 2–4 are typical. The application of the Reichardt (1951) approach would lead to a value of 4 (Kramm and Foken 1998).

The canopy resistance is often approximated as a stomatal resistance (Jarvis 1976):

$$r_c \approx r_{st} = \frac{r_{st,\min}\left(1 + \frac{b_{st}}{PAR}\right)}{g_\delta(\delta_e)\; g_\Psi(\Psi)\; g_T\left(T_f\right)\; g_C(c_{CO_2})\; g_D} \tag{5.42}$$

Thus, the parameterization depends primarily on the minimal stomatal resistance (Table 5.8) and the photosynthetically active radiation (PAR) with empirical constant b_{st}. The correction functions in the denominator of Eq. (5.44) have values from 0 to 1, and include the saturation deficit between the atmosphere and leafs (δ_e), the water stress (Ψ), the leaf temperature (T_f), and the local carbon dioxide concentration (c_{CO2}). Furthermore, g_D is a correction factor for the molecular diffusivity of different gases. Current model approaches are often based on the works of Farquhar et al. (1980) and Ball et al. (1987) with modifications by Leuning (1995). The parameterizations are very complicated, and are essentially independent models (Falge et al. 1997; Blümel 1998; Müller 1999; Jacobson 2005). A detailed description of these models is beyond the scope of this textbook and the reader is referred to the literature (Moene and van Dam 2014; Monson and Baldocchi 2014).

5.4 Modelling of Water Surfaces

It is generally easier to model the energy and matter exchange over water surfaces than over land surfaces (Smith et al. 1996; Geernaert 1999; Csanady 2001). However, methods for high wind velocities (>20 m s^{-1}) are very inaccurate. The usual approaches are comparable with bulk approaches (see Sect. 4.1.1). Thus, Eqs. (4.1)–(4.3) can be directly used for the open ocean where water and air temperatures became more similar, and a nearly-neutral stratification occurs. Otherwise it is recommended to use the profile equations with universal functions. Furthermore, the influence of surface waves should be included with the roughness-Reynolds number (Rutgersson and Sullivan 2005), see Eq. 3.3. A well-verified approach was

given by Panin (1985), in which Eqs. (4.2) and (4.3) are multiplied by the following factors respectively:

$$\cdot \left\{ \begin{array}{ll} (1 - z/L) \left[1 + 10^{-2} (z_0 \, u_* / \nu)^{3/4}\right] & z/L < 0 \\ [1/(1 + 3.5 \, z/L)] \left[1 + 10^{-2} (z_0 \, u_* / \nu)^{3/4}\right] & z/L > 0 \end{array} \right\} \tag{5.43}$$

The Stanton and Dalton numbers are those for neutral stratification.

Along the same line, the approaches used in hydrodynamics can also be applied over water bodies. For example Eq. (5.28) can be inserted in Eq. (4.2) instead of the product $u \; C_H$ and in Eq. (4.3) instead of the product $u \; C_E$.

These approaches fail for shallow water bodies. For shallow lakes the fluxes can be calculated from the temperature regime (Jacobs et al. 1998). However, the approaches given above can be applied assuming that over flat water the exchange is increased by steep waves and better mixing of the water body. According to Panin et al. (1996a) a correction function dependent on the water depth and the wave height should be included to determine fluxes in shallow water areas (depth lower than 20 m)

$$\begin{aligned} {Q_H}^{SW} &\approx Q_H (1 + 2h/H), \\ {Q_E}^{SW} &\approx Q_E (1 + 2h/H), \end{aligned} \tag{5.44}$$

where H is the water depth and h the wave height, which can be calculated using

$$h \approx \frac{0.07 \; {u_{10}}^2 \left(gH/{u_{10}}^2\right)^{3/5}}{g}, \tag{5.45}$$

where u_{10} is the wind velocity measured at 10 m (Davidan et al. 1985). This approach is also well verified for German lakes (Panin et al. 2006).

5.5 Boundary Layer Modelling

The determination of profiles of meteorological parameters for the entire boundary layer and of the mixed-layer height are the main objectives of atmospheric boundary layer models. Such models recently attracted increased interest due to wind power applications. Prognostic calculations of the mixed-layer height, which are feasible for the convective boundary layer, play also important roles when planning field experiments and can provide valuable guidance to observational meteorologists. There is a lot of literature related to this subject, and Seibert et al. (2000) and Hess (2004) give good overview papers.

5.5.1 Prognostic Models for the Mixed Layer Height

Prognostic equations for the mixed layer height go back to Tennekes (1973), who determined this height based on a sudden increase of the virtual potential temperature $\Delta\theta_v$. Furthermore, he postulated a small downward sensible heat flux and a change of the virtual potential temperature in the boundary layer (index BL). Above the mixed layer stable stratification with a lapse rate of γ is assumed:

$$\frac{d\Delta\theta_v}{dt} = \gamma \frac{dz_i}{dt} - \left(\frac{d\theta_v}{dt}\right)_{BL} \tag{5.46}$$

Defining an entrainment velocity w_e, the buoyancy flux at the mixed layer height is given by:

$$\left(\overline{w'\theta'_v}\right)_i = -w_e \Delta\theta_v. \tag{5.47}$$

To solve these equations a linear dependence between the buoyancy flux at mixed layer height and at the surface is assumed:

$$-\left(\overline{w'\theta'_v}\right)_i = A\left(\overline{w'\theta'_v}\right)_s, \tag{5.48}$$

whereby the entrainment parameter A assumes values between 0 and 1 (Seibert et al. 2000). Using these assumptions, a simple relationship follows:

$$\frac{dz_i}{dt} = A \frac{\left(\overline{w'\theta'_v}\right)_s}{\gamma z_i} \tag{5.49}$$

Instead of A often also $(1 + A)$ is used. This relationship is called bulk or slab model, and it reliably predicts the development of the boundary layer until noon. Required input parameters are the buoyancy flux at the ground and the lapse rate γ in the free atmosphere which can be estimated the morning radio sounding. If the buoyancy flux and lapse rate are constant in time, the integration of Eq. (5.49) yields (Stull 1988):

$$z_i^2 - z_{i_0}^2 = \frac{2A}{\gamma}\left(\overline{w'\theta'_v}\right)_s (t - t_0) \tag{5.50}$$

More complicated parameterizations are also available (Batchvarova and Gryning 1991; Rigby et al. 2015).

5.5.2 Parametrization of the Wind Profile in the Boundary Layer

The closure approaches discussed in Sect. 2.1.3 form the basis for the determination of the wind profile in the entire boundary layer. Therefore, the change of the wind velocity with height is given by first order closure according to Eq. (2.29) and the turbulent diffusion coefficient according to Eq. (2.38):

$$\frac{\partial u}{\partial z} = \frac{u_*}{\kappa \cdot l}. \tag{5.51}$$

Contrary to Eq. (2.36), the mixing length l is defined as $l = z$ not as $l = \kappa z$ (i.e. the von-Kármán constant is ignored here). This approach, which is valid in the surface layer, can be extended for the boundary layer by assuming that the friction velocity increases exponentially with height

$$u_*(z) = u_{*0}(1 - z/z_i)^{\alpha}, \tag{5.52}$$

whereby values for the exponent α discussed by various authors are given in Table 5.12. The mixing length can also be extended for the entire boundary layer (Arya 2001):

$$\frac{\partial u}{\partial z} = \frac{u_{*0}(1 - z/z_i)^{\alpha}}{\kappa}\left(\frac{1}{l_{SL}} + \frac{1}{l_{MBL}} + \frac{1}{l_{UBL}}\right) \tag{5.53}$$

Thereby $l_{SL} = z$ is the mixing length in the surface layer and l_{MBL} and l_{UBL} are the mixing lengths in the middle and upper boundary. With the assumption $\alpha = 1$ and a mixing length for the upper boundary layer it follows

$$\frac{\partial u}{\partial z} = \frac{u_{*0}}{\kappa}(1 - z/z_i)\left(\frac{1}{z} + \frac{1}{l_{MBL}} + \frac{1}{(z_i - z)}\right). \tag{5.54}$$

Table 5.12 Exponent of the vertical profile of the friction velocity in the atmospheric boundary layer according to Eq. (5.52)

Author	α
Panofsky (1973)	1.0 (neutral, from geostrophic drag coefficients)
Yokoyama et al. (1979)	0.5–1.5
Stull (1988)	0.5–1.0 (stabil) 0.5 (neutral) 0.5 (unstable, with additional term in Eq. 5.52)
Zilitinkevich u. Esau (2005)	0.75 (from LES-modelling)
Gryning et al. (2007)	1.0 (simplified assumption)

The determination of the mixing length l_{MBL} in the middle boundary layer remains a challenging problem. Gryning et al. (2007) used a resistance law (Gl. 2.145) which yields

$$\frac{1}{l_{MBL}} = \frac{2}{z_i}\left\{\left[\left(ln\frac{u_{*0}}{fz_0} - B\right)^2 + A^2\right]^{1/2} - ln\frac{z_i}{z_0}\right\} \tag{5.55}$$

with $A = 4.9$ and $B = 1.9$ (Zilitinkevich and Esau 2005). These equations are valid for the neutral boundary layer but they can be extended to the diabatic boundary layer by application of the universal functions of the surface layer and by assuming a dependence of A and B on the stability parameter μ (Eq. 2.143). The wind profile follows by integration of Eq. (5.54) and consideration of Eq. (5.57) (Gryning et al. 2007; Peña et al. 2010). These authors could show that the models give satisfactory results for homogeneous surfaces.

5.6 Modeling in Large-Scale Models

The modeling of the momentum, energy, and matter exchange in global circulation models is very simple in comparison to resistance models (Brutsaert 1982; Beljaars and Viterbo 1998; Zilitinkevich et al. 2002; Jacobson 2005). The limited computer time does not allow the application of complicated and iterative methods. The determination of the momentum and energy exchange uses bulk approaches (see Sect. 4.1.1), which are calculated for the layer between the surface (index s) and the first model layer (index 1). The surface fluxes are then given by:

$$u_*^2 = C_m\left|\overrightarrow{u_1}\right|^2 \tag{5.56}$$

$$\left(\overline{w'\theta'}\right)_0 = C_h\left|\overrightarrow{u_1}\right|(\theta_s - \theta_1) \tag{5.57}$$

$$\left(\overline{w'q'}\right)_0 = C_q\left|\overrightarrow{u_1}\right|(q_s - q_1) \tag{5.58}$$

In these equations, constant fluxes between the surface and the first model level (i.e. 30 m) are assumed. In the case of stable stratification, this assumption is questionable. The transfer coefficients $C_{m,h,q}$ can be calculated according to an approach by Louis (1979) or using a modified form proposed by Louis et al. (1982) with the coefficient for neutral stratification $C_{mn,hn,qn}$ and correction factors that are functions of atmospheric stability and the roughness of the underlying surface:

$$C_m = C_{mn}\, F_m\,(Ri_B, z_1/z_0) \tag{5.59}$$

$$C_h = C_{hn}\, F_h(Ri_B, z_1/z_0, z_1/z_{0T}) \tag{5.60}$$

$$C_q = C_{qn}\, F_q\left(Ri_B, z_1/z_0, z_1/z_{0q}\right) \tag{5.61}$$

In the neutral case, the transfer coefficients depend only on the roughness length (Eq. 4.5):

$$C_{mn} = \left(\frac{\kappa}{\ln \frac{z_1+z_0}{z_0}}\right)^2 \tag{5.62}$$

C_{hn} and C_{qn} can be determined according to Eq. (4.2) with z_{0T} and Eq. (4.3) with z_{0q}.

The bulk-Richardson number, Ri_B is given by:

$$Ri_B = \frac{g}{\theta_v}\,\frac{\theta_{v1} - \theta_{vs}}{\left|\overrightarrow{u_1}\right|^2} \tag{5.63}$$

Based on a limited number of experimental data (Louis 1979; Louis et al. 1982) the original expressions for the correction functions were derived as

$$F_m = \left(\frac{1 + 2\,b\,Ri_B}{\sqrt{1 + d\,Ri_B}}\right)^{-1}, \tag{5.64}$$

$$F_h = \left(\frac{1 + 3\,b\,Ri_B}{\sqrt{1 + d\,Ri_B}}\right)^{-1}, \tag{5.65}$$

where the empirical parameters are $b = 5$ and $d = 5$. Although these methods have been questioned (Beljaars and Holtslag 1991), they remain in use. Some corrections regarding the stability functions (Högström 1988) are sometimes used. However, the potential of modern micrometeorology is to a large extend not exhausted. An important criticism on the use of the Louis-(1979)-scheme is the application of roughness lengths for scalars. Their physical meaning is controversial, and they are nearly identical with the aerodynamic roughness length. Above the ocean, the roughness is determined according to either the Charnock equation or preferrably by a combination approach (see Sect. 2.3.2 and Table 2.8). The roughness lengths for scalars are parameterized according to the Roll (1948) approach for smooth surfaces (Beljaars 1995):

$$z_{0T} = 0.40\frac{\nu}{u_*}, \quad z_{0q} = 0.62\frac{\nu}{u_*} \tag{5.66}$$

For a better consideration of convective cases (Beljaars 1995) the wind vector can be enhanced by a gustiness component

$$\left|\overrightarrow{u_1}\right| = \left(u_1^2 + v_1^2 + \beta\, {w_*}^2\right)^{1/2} \tag{5.67}$$

with $\beta = 1$. The Deardorff velocity scale w_* (Eq. 2.43) can be simplified with the use of a mixed layer height of $z_i = 1$ km. This approach is in good agreement with experimental data, and represents the moisture exchange well.

The parameterization of stable stratification is especially difficult, as atmospheric stability may not be constant within the first model layer, the universal functions are not well defined, and the dynamics of the stable surface layer depends on external, larger scale parameters (Zilitinkevich and Mironov 1996; Handorf et al. 1999). In the simplest case, modified correction functions Eqs. (5.64) and (5.65) can be assumed (Louis et al. 1982)

$$F_m = \frac{1}{1 + 2\,b\,Ri_B\,(1 + d\,Ri_B)^{-1/2}}, \tag{5.68}$$

$$F_h = \frac{1}{1 + 3\,b\,Ri_B\,(1 + d\,Ri_B)^{1/2}} \tag{5.69}$$

with $b = 5$ and $d = 5$.

A parameterization applying external parameters was presented by Zilitinkevich and Calanca (2000)

$$F_m = \left(\frac{1 - \alpha_u\, Fi_0}{1 + \frac{C_u}{\ln z/z_0}\frac{z}{L}}\right)^2, \tag{5.70}$$

$$F_h = \left(\frac{1 - \alpha_\theta\, Fi\,\frac{Fi_0^2}{Ri_B}}{1 + \frac{C_\theta}{\ln z/z_0}\frac{z}{L}}\right), \tag{5.71}$$

where Fi is the inverse Froude-number and Fi_0 the inverse external Froude-number

$$Fi_0 = \frac{N\,z}{u} \tag{5.72}$$

where N is the Brunt-Väisälä frequency (Eq. 3.35), $C_u = \alpha_u \kappa / C_{uN}$, and $C_\theta = \alpha_\theta {Pr_t}^{-1} \kappa / C_{\theta N}$. The first experimental assessments of the coefficients are given in Table 5.13.

Table 5.13 Constants of the parameterization according to Zilitinkevich and Calanca (2000) in Eqs. (5.70) and (5.71)

Author	Experiment	C_{uN}	$C_{\theta N}$
Zilitinkevich and Calanca (2000)	Greenland experiment (Ohmura et al. 1992)	0.2…0.5	
Zilitinkevich et al. (2002)	Greenland experiment (Ohmura et al. 1992)	0.3	0.3
Zilitinkevich et al. (2002)	Cabauw tower, The Netherlands	0.04…0.9	
Sodemann and Foken (2004)	FINTUREX, Antarctica (Foken 1996), *Golden days*	0.51 ± 0.03	0.040 ± 0.001
Sodemann and Foken (2004)	FINTUREX, Antarctica (Foken 1996)	2.26 ± 0.08	0.022 ± 0.002

5.7 Large-Eddy Simulation

The model approaches discussed up to here have been primarily based on mean relations and averaged input parameters. They do not allow a spectral-dependent view, where the effects of single eddies can be shown. The reasons for this are the significant difficulties in spectral modeling and the large range of scales in atmospheric boundary layers. The spatial scale extends from the mixed layer height of about 10^3 m down to the Kolmogorov micro scale

$$\eta = \left(v^3/\varepsilon\right)^{1/4} \tag{5.73}$$

of about 10^{-3} m. The energy dissipation, ε, is identical with the energy input from the energy conserving scale $l \sim z_i$ and the relevant characteristic velocity:

$$\varepsilon = u^3/l \tag{5.74}$$

For the convective boundary layer, the energy dissipation is approximately 10^{-3} m^2 s^{-3}. The turbulent eddies in the atmospheric boundary layer cover a range from kilometers to millimeters. Thus, a numerical solution of the Navier-Stokes equation would need 10^{18} grid points. Because the large eddies, which are easily resolvable in a numerical model, are responsible for the transports of momentum, heat and moisture, it is necessary to estimate the effects of the small dissipative eddies which are not easily resolvable. The simulation technique for large eddies (Large-Eddy-Simulation: LES) consists in the modeling of the important contributions of the turbulent flow and to parameterize integral effects of small eddies (Moeng 1998). For technical applications with low Reynolds numbers, almost all eddy sizes can be resolved. The latter method is called Direct Numerical Simulation (DNS).

The basic equations for LES are the Navier-Stokes equations, where single terms must be transferred into volume averages

$$\tilde{u}_i = \iiint (u_i\, G)\, dx\, dy\, dz\,, \tag{5.75}$$

where G is a filter function which filters out small eddies and regards only large eddies. The total contribution of the small eddies is taken into account in an additional term of the volume averaged Navier-Stokes equations and parameterized with a special model. The widely used approach is the parameterization according to Smagorinsky-Lilly (Smagorinsky 1963; Lilly 1967), where the diffusion coefficient is described in terms of the wind and temperature gradients. For small eddies in the inertial subrange, the −5/3 law is assumed so that the relevant constants can be determined (Moeng and Wyngaard 1989). If small-scale phenomena have an important influence, the application of LES modeling requires a lot of care, for example, near the surface or when including chemical reactions.

The LES technique is currently no longer just a research tool, which allows investigating simple situations with high resolution in space and time, but at the cost of large computation times. Results from LES studies led to significant advancements in the understanding of the atmospheric boundary layer. Beginning with the first simulations by (Deardorff 1972), LES has been mainly applied to the convective boundary layer (Schmidt and Schumann 1989; Schumann 1989). In most cases, the ground surface is assumed homogeneous or only simply structured. Recently, the stably stratified boundary layer has become a topic of investigations. In the last 20 years, LES is a rapidly developing research field with many publications (Garratt 1992; Moeng 1998; Kantha and Clayson 2000; Raasch and Schröter 2001, Moeng et al. 2004, and others). Increasingly, heterogeneous surfaces like forests (Kanani-Sühring and Raasch 2015; Schlegel et al. 2015), valleys (Brötz et al. 2014), urban areas (Letzel et al. 2008) are modelled, and technical applications related to the use of wind power (Vollmer et al. 2015) are becoming common.

5.8 Area Averaging

All methods to determine the turbulent momentum and energy fluxes are related to the surface above which the fluxes are measured. But in most cases, the problem is to determine for example the evapotranspiration within a catchment, or over a large agricultural area or even over entire landscapes. Area-averaged fluxes are necessary in numerical weather and climate forecast models as input or validation parameters. It is impossible to calculate them by a simple averaging of the input parameters because complicated non-linear relations could cause large errors. Nevertheless this method has recently been used for weather and climate models, which use simple parameterizations of the interaction of the atmosphere with the surface.

Using the resistance concept in the form of Eq. (5.30), the total resistance of the area is a *parallel connection* of the total resistances of areas with different land use:

$$\frac{1}{r_g} = \frac{1}{r_{g1}} + \frac{1}{r_{g2}} + \frac{1}{r_{g3}} + \cdots \tag{5.76}$$

Applying the method of parameter aggregation, it follows from Eq. (5.76) for an averaging of individual resistances as in Eq. (5.32):

$$\frac{1}{r_g} = \frac{1}{\frac{1}{N}\sum_i r_{a_i}} + \frac{1}{\frac{1}{N}\sum_i r_{mt_i}} + \frac{1}{\frac{1}{N}\sum_i r_{c_i}} \tag{5.77}$$

It is immediately clear that Eq. (5.77) is physically incorrect. Nevertheless this approach is practicable because, for example, the mean resistance of the turbulent layer can be determined by averaging the roughness lengths of individual areas as it is done in most of weather prediction and climate models. However, one must be aware that because of non-linear relations significant estimation errors of the turbulent fluxes can occur (Stull and Santoso 2000).

In contrast, for the flux aggregation the total resistance must be calculated for each individual area, which also implies different boundary conditions for the different areas:

$$\frac{1}{r_g} = \sum_i \frac{1}{r_{a_i} + r_{mt_i} + r_{c_i}} \tag{5.78}$$

The more simple methods of flux averaging differ in the ways Eq. (5.78) is used for the individual areas.

An overview about different area averaging methods is given in Table 5.14. In this table statistical-dynamical methods, which give only a rough resolution of the land use types, are not mentioned.

The area averaging is also important for the experimental determination of turbulent fluxes, because different land use types are often in the footprint of the sensors, which generates a mixed signal. This problem can be solved if additional measurements are taken for parts of the area, which allows a footprint dependent correction (Göckede et al. 2005; Leclerc and Foken 2014). In a similar way, the correction can be determined if at least for one part of the area the fluxes are modelled (Biermann et al. 2014).

5.8.1 Simple Area Averaging Methods

A very simple, but still-used method is the calculation of fluxes for dominant areas. For each grid element of a numerical model, the dominate land use must be

Table 5.14 Methods of area averaging

Averaging method	Procedure	Example/reference
Parameter aggregation	Averaging for example of the roughness length	$\overline{z_0} = \frac{1}{N}\sum_{i}^{N} z_{0i}$
	Averaging of *effective* parameters	i.e. Troen and Lundtang Peterson (1989), see Sect. 3.1.1
Flux aggregation	Averaging for example of the roughness length with Fourier analysis	Hasager and Jensen (1999), Hasager et al. (2003)
	Mixing method for resistances	Mölders et al. (1996), Mölders (2012)
	Flux determination for dominant areas	Avissar and Pielke (1989)
	Mosaic approach	Mölders et al. (1996), Mölders (2012)
	• *tile* approach	
	• subgrid approach	

determined over which the fluxes are calculated. It is assumed that over all grid elements the different land uses are statistically balanced. Therefore, each grid element has only one land use type. The averaging within a grid element is a quasi parameter-averaging process because the individual estimations of the parameters of the grid elements are largely intuitive and therefore parameter averaged.

The *blending-height* concept (see Sect. 3.2.4) can also be used for area averaging. It is assumed that at a certain height above the ground (for example 50 m) the fluxes above the heterogeneities of the surface do not differ and can be presented as an averaged flux. The fluxes for this height can be parameterized using effective parameters. A typical case is the application of effective roughness length, where the friction velocities are averaged instead of the roughness lengths (Taylor 1987; Blyth 1995; Schmid and Bünzli 1995a, 1995b; Mahrt 1996; Hasager and Jensen 1999; Hasager et al. 2003). From Eq. (2.60), it follows that by averaging the friction velocities of the individual areas an effective roughness length is given by:

$$z_{0eff} = \frac{\overline{u_* \ln z_0}}{\overline{u_*}} \tag{5.79}$$

A more empirical averaging of roughness lengths as presented by Troen and Lundtang Petersen (1989) for the European Wind Atlas (Table 3.1) can be classified as an early stage of the above given method. A good effective averaging is of increasing importance for many practical reasons, for example micrometeorological processes in the urban boundary layer (Grimmond et al. 1998).

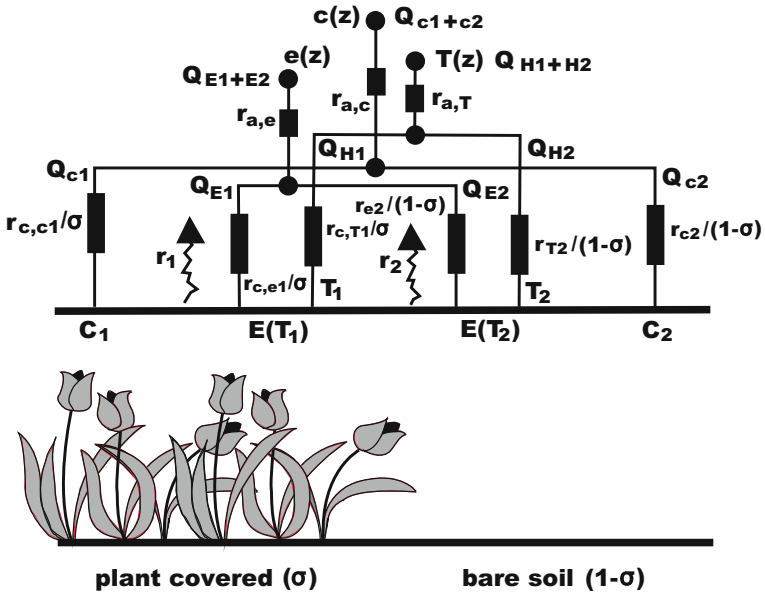

Fig. 5.5 Schematic representation of the mixing method (modified according to Mölders 2012, with kind permission of © Springer Berlin, Heidelberg 2012, All rights reserved)

The procedure of roughness averaging with an effective roughness length is widely applied in the determination of turbulent resistances. In a mixing method, only those resistances are averaged which are obviously different for the different individual areas. Generally, uniform values are assumed for the turbulent and the molecular-turbulent resistances, and only the canopy resistance is averaged according—comparable with the mosaic approach (see Sect. 5.8.2)—to the land use (Fig. 5.5). This method uses the fact that in most cases meteorological information is not available for different land uses within a grid element. However, for the determination of the turbulent and molecular-turbulent resistances a parameter averaging is used because these are often not parameterized for a specific underlying surface.

5.8.2 *Complex Area-Averaging Methods*

The mosaic approach belongs to the complex methods (Avissar and Pielke 1989; Mölders et al. 1996). This description is currently often used as a generic term for different applications. In the simplest case, (*tile*-approach) for each grid cell, contributions of similar land use types are combined and the parameterization of all resistances and the fluxes for each type will be separately calculated. The mean flux

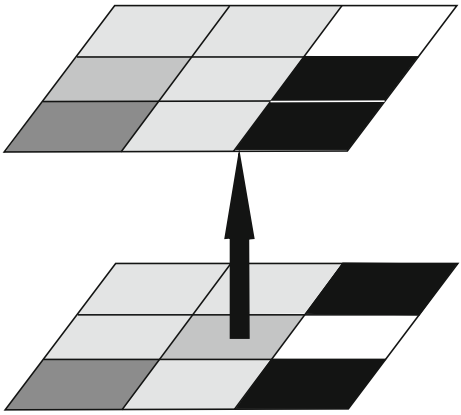

Fig. 5.6 Schematic representation of the mosaic approach (Mölders et al. 1996). The initial distribution of the surface structures will be combined according their contributions for further calculations. Adapted with kind permission of

is the weighted average according to the contribution of the single land uses (Fig. 5.6):

$$Q_x = \sum_{i=1}^{N} a_i Q_{xi} \tag{5.80}$$

whereby Q_x is the averaged flux and Q_{xi} are the fluxes of partial areas with an area fraction of a_i. This method is widely used for high-resolution models in space (100 m grid size), but it does not allow horizontal fluxes (advection) between the areas.

This disadvantage is overcome with the subgrid method (Fig. 5.7)

$$Q_x = \frac{1}{N} \sum_{i=1}^{N} Q_{xi} \tag{5.81}$$

where for each land use a small multi-layer model is used, which takes advection into account. For a certain height according to the blending-height concept, an average of the fluxes for a grid element is assumed. Such models correspond well with the reality, but they require very large computer capacity. Therefore, the subgrid method has been applied only for single process studies.

Model calculations with subgrid models and experiments (Panin et al. 1996b; Klaassen et al. 2002) show that fluxes above one surface are not independent of the neighbourhood surfaces. Accordingly, these model studies for highly heterogeneous surfaces show an increase of the flux for the total area (Friedrich et al. 2000). According to numerical studies by Schmid and Bünzli (1995a) this increase of the fluxes occurs on the lee side of boundaries between the single surfaces (Fig. 5.8).

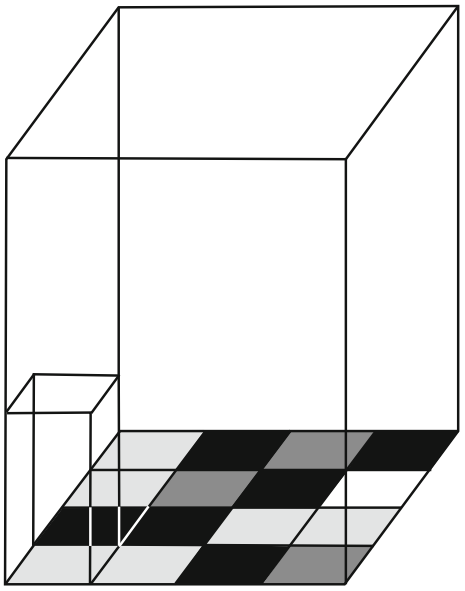

Fig. 5.7 Schematic representation of the subgrid method (Mölders et al. 1996). The surface structure will be used further on for selected model calculations. Adapted with kind permission of © Author(s) 1996, CC Attribution 4.0 Licence, All rights reserved

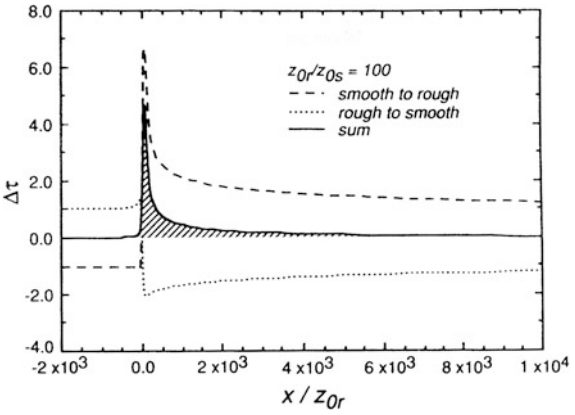

Fig. 5.8 Ratio of the friction velocities ($\Delta\tau = \tau_r/\tau_s$) above both surfaces for the flow over the roughness change. Immediately after the roughness change an increase of the friction velocity is observed. (Schmid and Bünzli 1995a, published with kind permission of © Royal Meteorological Society Reading 1995, All rights reserved)

5.8.3 Model Coupling

Averaging concepts are often used in the coupling of models. For model coupling, different approaches have been tested and are promising (Mölders 2001). The simplest versions are the direct data transfer and the one-way coupling, where the plant, soil, or hydrological model (SVAT and others) get their forcing from a meteorological model. In a two-way coupling, the SVAT model for example, gives its calculated fluxes back to the meteorological model. If sufficient computer time is available, then complete couplings are possible.

Instead of a coupling with effective parameters, a coupling with fluxes is preferred (Best et al. 2004), because effective parameters cannot adequately describe the high non-linearity of the fluxes. Instead of a coupling with area-averaged fluxes (Herzog et al. 2002), modules between the models should be included (Mölders 2001), which allow suitable coupling of the heterogeneous surface in different models, e.g. an averaging according to the mosaic or subgrid approach (Mölders et al. 1996; Albertson and Parlange 1999). It very important that the coupled models use consistent parameterizations (Mölders and Kramm 2014). This issue is relevant for the development of Earth system models, which are discussed in climate research.

For model coupling, an unsolved problem is the usage sufficient grid structures. Meteorological models are based on rectangular grids, while land use models are based on polygons. A promising development is the use of adaptive grids (Behrens et al. 2005) that fit themselves to the respective surface conditions of each model, and have a high resolution in regions where the modeling is very critical or where the largest heterogeneities occur.

References

Albertson JD and Parlange MB (1999) Natural integration of scalar fluxes from complex terrain. Adv Water Res. 23:239–252.

Allen RG, Pereira LS, Raes D and Smith M (1998) Crop evaporation. FAO Irrigation Drainage Pap. 56:XXVI + 300 pp.

Allen RG, Walter IA, Elliott R, Howell T, Itenfisu D and Jensen M (2005) The ASCE standardized reference evapotranspiration equation. Environmental and Water Resources Institute of the American Society of Civil Engineers, X + 59 pp.

Arya SP (2001) Introduction to Micrometeorology. Academic Press, San Diego, 415 pp.

Avissar R and Pielke RA (1989) A parametrization of heterogeneous land surface for atmospheric numerical models and its impact on regional meteorology. Monthly Weather Review. 117:2113–2136.

Baldocchi D (1988) A multi-layer model for estimating sulfor dioxid deposition to a deciduous oke forest canopy. Atmos Environm. 22:869–884.

Baldocchi D, Hicks BB and Camara P (1987) A canopy stomatal resistance model for gaseous deposition to vegetated surfaces. Atmos Environm. 21:91–101.

Ball JT, Woodrow IE and Berry JA (1987) A model predicting stomatal conductance and its contribution to the control of photosynthesis under different environmental conditions. In: Biggens J (ed.), Progress in Photosynthesis Research. Vol. IV. Martinus Nijhoff Publisher, Dordrecht, IV.5.221–IV.5.224.

Batchvarova E and Gryning S-E (1991) Applied model for the growth of the daytime mixed layer. Boundary-Layer Meteorol. 56:261–274.

Behrens J, Rakowsky N, Hiller W, Handorf D, Läuter M, Päpke J and Dethloff K (2005) amatos: parallel adaptive mesh generator for atmospheric and oceanic simulation. Ocean Modelling. 10:171–183.

Beljaars ACM (1995) The parametrization of surface fluxes in large scale models under free convection. Quart J Roy Meteorol Soc. 121:255–270.

Beljaars ACM and Holtslag AAM (1991) Flux parametrization over land surfaces for atmospheric models. J Appl Meteorol. 30:327–341.

Beljaars ACM and Viterbo P (1998) Role of the boundary layer in a numerical weather prediction model. In: Holtslag AAM and Duynkerke PG (eds.), Clear and Cloudy Boundary Layers, vol VNE 48. Royal Netherlands Academy of Arts and Sciences, Amsterdam, 287–304.

Best MJ, Beljaars A, Polcher J and Viterbo P (2004) A proposed structure for coupling tiled surfaces with the planetary boundary layer. J Hydrometeorol. 5:1271–1278.

Biermann T, Babel W, Ma W, Chen X, Thiem E, Ma Y and Foken T (2014) Turbulent flux observations and modelling over a shallow lake and a wet grassland in the Nam Co basin, Tibetan Plateau. Theor Appl Climat. 116:301–316.

Bjutner EK (1974) Teoreticeskij rascet soprotivlenija morskoj poverchnosti (Theoretical calculation of the resistance at the surface of the ocean). In: Dubov AS (ed.), Processy perenosa vblizi poverchnosti razdela okean - atmosfera (Exchange processes near the ocean - atmosphere interface). Gidrometeoizdat, Leningrad, 66–114.

Blackadar AK (1997) Turbulence and Diffusion in the Atmosphere. Springer, Berlin, Heidelberg, 185 pp.

Blümel K (1998) Estimation of sensible heat flux from surface temperature wave and one-time-of-day air temperature observations. Boundary-Layer Meteorol. 86:193–232.

Blyth EM (1995) Comments on 'The influence of surface texture on the effective roughness length' by H. P. Schmid and D. Bünzli (1995, **121**, 1–21). Quart J Roy Meteorol Soc. 121:1169–1171.

Brötz B, Eigenmann R, Dörnbrack A, Foken T and Wirth V (2014) Early-morning flow transition in a valley in low-mountain terrain. Boundary-Layer Meteorol. 152:45–63.

Brutsaert WH (1982) Evaporation into the atmosphere: Theory, history and application. D. Reidel, Dordrecht, 299 pp.

Burridge DM and Gadd AJ (1977) The Meteorological Office operational 10-level numerical weather prediction model (December 1975). Meteorological Office Technical Notes. 34:39 pp.

Csanady GT (2001) Air-sea interaction, Laws and mechanisms. Cambridge University Press, Cambridge, New York, 239 pp.

Davidan IN, Lopatuhin LI and Rogkov VA (1985) Volny v okeane (Waves in the ocean). Gidrometeoizdat, Leningrad, 256 pp.

Deardorff JW (1972) Numerical investigation of neutral und unstable planetary boundary layer. J Atmos Sci. 29:91–115.

DeBruin HAR (1983) A model for the Priestley–Taylor parameter α. J Climate Appl Meteorol. 22:572–578.

DeBruin HAR and Holtslag AAM (1982) A simple parametrization of the surface fluxes of sensible and latent heat during daytime compared with the Penman–Monteith concept. J Climate Appl Meteorol. 21:1610–1621.

Dommermuth H and Trampf W (1990) Die Verdunstung in der Bundesrepublik Deutschland, Zeitraum 1951-1980, Teil 1. Deutscher Wetterdienst, Offenbach, 10 pp.

Doorenbos J and Pruitt WO (1977) Guidelines for predicting crop water requirements. FAO Irrigation Drainage Pap. 24, 2nd ed.:145 pp.

DVWK (1996) Ermittlung der Verdunstung von Land- und Wasserflächen. DVWK-Merkblätter zur Wasserwirtschaft. 238:134 pp.

Falge EM, Ryel RJ, Alsheimer M and Tenhunen JD (1997) Effects on stand structure and physiology on forest gas exchange: A simulation study for Norway spruce. Trees. 11:436–448.

Farquhar GD, von Caemmerer S and Berry JA (1980) A biochemical of photosynthetic CO_2 assimilation in leaves of C_3 species. Planta. 149:78–90.

Foken T (1978) The molecular temperature boundary layer of the atmosphere over various surfaces. Archiv Meteorol Geophys Bioklim, Ser. A. 27:59–67.

Foken T (1984) The parametrisation of the energy exchange across the air-sea interface. Dynamics Atm Oceans. 8:297–305.

Foken T (1986) An operational model of the energy exchange across the air-sea interface. Z Meteorol. 36:354–359.

Foken T (1996) Turbulenzexperiment zur Untersuchung stabiler Schichtungen. Ber Polarforschung. 188:74–78.

Foken T (2002) Some aspects of the viscous sublayer. Meteorol Z. 11:267–272.
Foken T (2016) Angewandte Meteorologie. Springer-Spektrum, Berlin, Heidelberg, 394 pp.
Foken T, Kitajgorodskij SA and Kuznecov OA (1978) On the dynamics of the molecular temperature boundary layer above the sea. Boundary-Layer Meteorol. 15:289–300.
Foken T, Dlugi R and Kramm G (1995) On the determination of dry deposition and emission of gaseous compounds at the biosphere-atmosphere interface. Meteorol Z. 4:91–118.
Friedrich K, Mölders N and Tetzlaff G (2000) On the influence of surface heterogeneity on the Bowen-ratio: A theoretical case study. Theor Appl Climat. 65:181–196.
Garratt JR (1992) The Atmospheric Boundary Layer. Cambridge University Press, Cambridge, 316 pp.
Geernaert GL (ed) (1999) Air-Sea Exchange: Physics, Chemistry and Dynamics. Kluwer Acad. Publ., Dordrecht, 578 pp.
Göckede M and Foken T (2001) Ein weiterentwickeltes Holtslag-van Ulden-Schema zur Stabilitätsparametrisierung in der Bodenschicht. Österreichische Beiträge zu Meteorologie und Geophysik. 27:(Extended Abstract and pdf-file on CD) 210.
Göckede M, Markkanen T, Mauder M, Arnold K, Leps JP and Foken T (2005) Validation of footprint models using natural tracer measurements from a field experiment. Agrical Forest Meteorol. 135:314–325.
Grimmond CSB, King TS, Roth M and Oke TR (1998) Aerodynamic roughness of urban areas derived from wind observations. Boundary-Layer Meteorol. 89:1–24.
Groß G (1993) Numerical Simulation of Canopy Flows. Springer, Berlin, Heidelberg pp.
Gryning S-E, Batchvarova E, Brümmer B, Jørgensen H and Larsen S (2007) On the extension of the wind profile over homogeneous terrain beyond the surface boundary layer. Boundary-Layer Meteorol. 124:251–268.
Gusev EM and Nasonova ON (2010) Modelirovanie teplo- i vlagoobmena poverchnosti sushi s atmosferoj (Modelling of the heat and moisture exchange of land surfaces with the atmosphere). Nauka, Moskva, 327 pp.
Handorf D, Foken T and Kottmeier C (1999) The stable atmospheric boundary layer over an Antarctic ice sheet. Boundary-Layer Meteorol. 91:165–186.
Hasager CB and Jensen NO (1999) Surface-flux aggregation in heterogeneous terrain. Quart J Roy Meteorol Soc. 125:2075–2102.
Hasager CB, Nielsen NW, Jensen NO, Boegh E, Christensen JH, Dellwik E and Soegaard H (2003) Effective roughness calculated from satellite-derived land cover maps and hedge-information used in a weather forecasting model. Boundary-Layer Meteorol. 109:227–254.
Haude W (1955) Bestimmung der Verdunstung auf möglichst einfache Weise. Mitt Dt Wetterdienst. 11:24 pp.
Herzog H-J, Vogel G and Schubert U (2002) LLM - a nonhydrostatic model applied to high-resolving simulation of turbulent fluxes over heterogeneous terrain. Theor Appl Climat. 73:67–86.
Hess GD (2004) The neutral, barotropic planetary layer capped by a low-level inversion. Boundary-Layer Meteorol. 110:319–355.
Hicks BB, Baldocchi DD, Meyers TP, Hosker jr. RP and Matt DR (1987) A preliminary multiple resistance routine for deriving dry deposition velocities from measured quantities. Water, Air and Soil Pollution. 36:311–330.
Hillel D (1980) Applications of Soil Physics. Academic Press, New York, 385 pp.
Högström U (1988) Non-dimensional wind and temperature profiles in the atmospheric surface layer: A re-evaluation. Boundary-Layer Meteorol. 42:55–78.
Holtslag AAM and van Ulden AP (1983) A simple scheme for daytime estimates of the surface fluxes from routine weather data. J Climate Appl Meteorol. 22:517–529.
Houghton JT (2015) Global Warming, The complete Briefing. Cambridge University Press, Cambridge, 396 pp.

Inclán MG, Forkel R, Dlugi R and Stull RB (1996) Application of transilient turbulent theory to study interactions between the atmospheric boundary layer and forest canopies. Boundary-Layer Meteorol. 79:315–344.

Jacobs AFG, Heusinkveld BG and Nieveen JP (1998) Temperature behavior of a natural shallow water body during a summer periode. Theor Appl Climat. 59:121–127.

Jacobson MZ (2005) Fundamentals of Atmospheric Modelling. Cambridge University Press, Cambridge, 813 pp.

Jarvis PG (1976) The interpretation of the variations in leaf water potential and stomatal conductance found in canopies in the field. Phil Trans Roy. Soc London B: Biolog Sci. 273:593–610.

Kaimal JC and Finnigan JJ (1994) Atmospheric Boundary Layer Flows: Their Structure and Measurement. Oxford University Press, New York, NY, 289 pp.

Kanani-Sühring F and Raasch S (2015) Spatial variability of scalar concentrations and fluxes downstream of a clearing-to-forest transition: A Large-Eddy Simulation study. Boundary-Layer Meteorol. 155:1–27.

Kantha LH and Clayson CA (2000) Small scale processes in geophysical fluid flows. Academic Press, San Diego, 883 pp.

Kitajgorodskij SA and Volkov JA (1965) O rascete turbulentnych potokov tepla i vlagi v privodnom sloe atmosfery (The calculation of the turbulent fluxes of temperature and humidity in the atmosphere near the water surface) Izv AN SSSR, Fiz Atm Okeana. 1:1317–1336.

Klaassen W, van Breugel PB, Moors EJ and Nieveen JP (2002) Increased heat fluxes near a forest edge. Theor Appl Climat. 72:231–243.

Kramm G and Foken T (1998) Ucertainty analysis on the evaporation at the sea surface. Second Study Conference on BALTEX, Juliusruh, 25–29 May 1998. BALTEX Secretariat, pp. 113–114.

Kramm G, Foken T, Molders N, Muller H and Paw U KT (1996a) The sublayer-Stanton numbers of heat and matter for different types of natural surfaces. Contr Atmosph Phys. 69:417–430.

Kramm G, Beier M, Foken T, Müller H, Schröder P and Seiler W (1996b) A SVAT-skime for NO, NO_2, and O_3 - Model description and test results. Meteorol Atmos Phys. 61:89–106.

Kramm G, Dlugi R and Mölders N (2002) Sublayer-Stanton numbers of heat and matter for aerodynamically smooth surfaces: basic considerations and evaluations. Meteorol Atmos Phys. 79:173–194.

Landau LD and Lifschitz EM (1987) Fluid Mechanics. Butterworth-Heinemann, Oxford, 539 pp.

Leclerc MY and Foken T (2014) Footprints in Micrometeorology and Ecology. Springer, Heidelberg, New York, Dordrecht, London, XIX, 239 pp.

Letzel MO, Krane M and Raasch S (2008) High resolution urban large-eddy simulation studies from street canyon to neighbourhood scale. Atmos Environm. 42:8770–8784.

Leuning R (1995) A critical appraisal of a combined stomatal-photosynthesis model for C_3 plants. Plant, Cell & Environment. 18:339–355.

Lilly DK (1967) The representation of small-scale turbulence in numerical simulation experiments. In: Goldstein HH (ed). IBM Scientific Computing Symposium on Environmental Science, Yorktown Heights, N.Y., November 14-16, 1966 1967, pp. IBM Form No. 320-1951, 1195–1210.

Louis JF (1979) A parametric model of vertical fluxes in the atmosphere. Boundary-Layer Meteorol. 17:187–202.

Louis JF, Tiedtke M and Geleyn JF (1982) A short history of the PBL parametrization at ECMWF. Workshop on Boundary Layer parametrization, Reading1982. ECMWF, pp. 59–79.

Lüers J and Bareiss J (2010) The effect of misleading surface temperature estimations on the sensible heat fluxes at a high Arctic site – the Arctic Turbulence Experiment 2006 on Svalbard (ARCTEX-2006). Atmos Chem Phys. 10:157–168.

Mahrt L (1996) The bulk aerodynamic formulation over heterogeneous surfaces. Boundary-Layer Meteorol. 78:87–119.

Mallick K, Boegh E, Trebs I, Alfieri JG, Kustas WP, Prueger JH, Niyogi D, Das N, Drewry DT, Hoffmann L and Jarvis AJ (2015) Reintroducing radiometric surface temperature into the Penman–Monteith formulation. Water Resources Res. 51:6214–6243.

Mangarella PA, Chambers AJ, Street RL and Hsu EY (1972) Laboratory and field interfacial energy and mass flux and prediction equations. J Geophys Res. 77:5870–5875.

Mangarella PA, Chambers AJ, Street RL and Hsu EY (1973) Laboratory studies of evaporation and energy transfer through a wavy air-water interface. J. Phys. Oceanogr. 3:93–101.

Mengelkamp H-T, Warrach K and Raschke E (1999) SEWAB a parameterization of the surface energy and water balance for atmospheric and hydrologic models. Adv Water Res. 23:165–175.

Meyers TP and Paw U KT (1986) Testing a higher-order closure model for modelling airflow within and above plant canopies. Boundary-Layer Meteorol. 37:297–311.

Meyers TP and Paw U KT (1987) Modelling the plant canopy microenvironment with higher-order closure principles. Agrical Forest Meteorol. 41:143–163.

Mix W, Goldberg V and Bernhardt K-H (1994) Numerical experiments with different approaches for boundary layer modelling under large-area forest canopy conditions. Meteorol Z. 3:187–192.

Moene AF and van Dam JC (2014) Transport in the Atmosphere-Vegetation-Soil Continuum. Cambridge University Press, Cambridge, 436 pp.

Moeng C-H (1998) Large eddy simulation of atmospheric boundary layers. In: Holtslag AAM and Duynkerke PG (eds.), Clear and cloudy boundary layers, vol VNE 48. Royal Netherlands Academy of Arts and Science, Amsterdam, 67–83.

Moeng C-H and Wyngaard JC (1989) Evaluation of turbulent transport and dissipation closure in second-order modelling. J Atmos Sci. 46:2311–2330.

Moeng C-H, Sullivan PP and Stevens B (2004) Large-eddy simulation of cloud-topped mixed layers. In: Fedorovich Eet al (eds.), Atmospheric Turbulence and mesoscale Meteorology. Cambridge University Press, Cambridge, 95–114.

Mölders N (2001) Concepts for coupling hydrological and meteorological models. Wiss. Mitt. aus dem Inst. für Meteorol. der Univ. Leipzig und dem Institut für Troposphärenforschung e. V. Leipzig. 22:1–15.

Mölders N (2012) Land-Use and Land-Cover Changes, Impact on climate and air quality. Springer, Dordrecht, Heidelberg, London, New York, 189 pp.

Mölders N and Kramm G (2014) Lectures in Meteorology. Springer, Cham Heidelberg New York Dordrecht London XIX, 591 pp.

Mölders N, Raabe A and Tetzlaff G (1996) A comparison of two strategies on land surface heterogeneity used in a mesoscale ß meteorological model. Tellus. 48A:733–749.

Monson R and Baldocchi D (2014) Terrestrial Biosphere-Atmosphere Fluxes. Cambridge University Press, New York, XXI, 487 pp.

Monteith JL (1965) Evaporation and environment. Symp Soc Exp Biol. 19:205–234.

Montgomery RB (1940) Observations of vertical humidity distribution above the ocean surface and their relation to evaporation. Pap Phys Oceanogr Meteorol. 7:1–30.

Müller C (1999) Modelling Soil-Biosphere Interaction. CABI Publishing, Wallingford, 354 pp.

Ohmura A, Steffen K, Blatter H, Greuell W, Rotach M, Stober M, Konzelmann T, Forrer J, Abe-Ouchi A, Steiger D and Neiderbäumer G (1992) Greenland Expedition, Progress Report No. 2, April 1991 to Oktober 1992. Swiss Federal Institute of Technology, Zürich, 94 pp.

Owen PR and Thomson WR (1963) Heat transfer across rough surfaces. J Fluid Mech. 15:321–334.

Panin GN (1985) Teplo- i massomen meszdu vodoemom i atmospheroj v estestvennych uslovijach (Heat- and mass exchange between the water and the atmosphere in the nature). Nauka, Moscow, 206 pp.

Panin GN, Nasonov AE and Souchintsev MG (1996a) Measurements and estimation of energy and mass exchange over a shallow see. In: Donelan M (ed.), The air-sea interface, Miami, 489–494.

Panin GN, Tetzlaff G, Raabe A, Schönfeld H-J and Nasonov AE (1996b) Inhomogeneity of the land surface and the parametrization of surface fluxes - a discussion. Wiss Mitt Inst Meteorol Univ Leipzig und Inst Troposphärenforschung Leipzig. 4:204–215.

Panin GN, Nasonov AE, Foken T and Lohse H (2006) On the parameterization of evaporation and sensible heat exchange for shallow lakes. Theor Appl Climat. 85:123–129.

Panofsky HA (1973) Tower micrometeorology. In: Haugen DA (ed.), Workshop on Micrometeorology. American Meteorological Society, Boston, 151–176.

Peña A, Gryning S-E and Hasager C (2010) Comparing mixing-length models of the diabatic wind profile over homogeneous terrain. Theor Appl Climat. 100:325–335.

Penman HL (1948) Natural evaporation from open water, bare soil and grass. Proceedings Royal Society London. A193:120–195.

Priestley CHB and Taylor JR (1972) On the assessment of surface heat flux and evaporation using large-scale parameters. Monthly Weather Review. 100:81–92.

Pyles RD, Weare BC and Paw U KT (2000) The UCD Advanced Canopy-Atmosphere-Soil Algorithm: comparisons with observations from different climate and vegetation regimes. Quart J Roy Meteorol Soc. 126:2951–2980.

Raasch S and Schröter M (2001) PALM - A large-eddy simulation model performing on massively parallel computers. Meteorol Z. 10:363–372.

Reichardt H (1951) Vollständige Darstellung der turbulenten Geschwindigkeitsverteilung in glatten Röhren. Z angew Math Mech. 31:208–219.

Richter D (1977) Zur einheitlichen Berechnung der Wassertemperatur und der Verdunstung von freien Wasserflächen auf statistischer Grundlage. Abh Meteorol Dienstes DDR. 119:35 pp.

Rigby JR, Yin J, Albertson J and Porporato A (2015) Approximate Analytical Solution to Diurnal Atmospheric Boundary-Layer Growth Under Well-Watered Conditions. Boundary-Layer Meteorol. 156:73–89.

Roll HU (1948) Wassernahes Windprofil und Wellen auf dem Wattenmeer. Ann Meteorol. 1:139–151.

Rutgersson A and Sullivan PP (2005) Investigating the effects of water waves on the turbulence structure in the atmosphere using direct numerical simulations. Dynamics Atm Oceans. 38:147–171.

Schädler G, Kalthoff N and Fiedler F (1990) Validation of a model for heat, mass and momentum exchange over vegetated surfaces using LOTREX-10E/HIBE88 data. Contr Atmosph Phys. 63:85–100.

Schlegel F, Stiller J, Bienert A, Maas H-G, Queck R and Bernhofer C (2015) Large-Eddy Simulation study of the effects on flow of a heterogeneous forest at sub-tree resolution. Boundary-Layer Meteorol. 154:27–56.

Schlichting H and Gersten K (2006) Grenzschicht-Theorie. Springer, Berlin, Heidelberg, 799 pp.

Schmid HP and Bünzli D (1995a) The influence of the surface texture on the effective roughness length. Quart J Roy Meteorol Soc. 121:1–21.

Schmid HP and Bünzli D (1995b) Reply to comments by E. M. Blyth on 'The influence of surface texture on the effective roughness length'. Quart J Roy Meteorol Soc. 121:1173–1176.

Schmidt H and Schumann U (1989) Coherent structures of the convective boundary layer derived from large eddy simulations. J Fluid Mech. 200:511–562.

Schrödter H (1985) Verdunstung, Anwendungsorientierte Meßverfahren und Bestimmungsmethoden. Springer, Berlin, Heidelberg, 186 pp.

Schumann U (1989) Large-eddy simulation of turbulent diffusion with chemical reactions in the convective boundary layer. Atmos Environm. 23:1713–1727.

Seibert P, Beyrich F, Gryning S-E, Joffre S, Rasmussen A and Tercier P (2000) Review and intercomparison of operational methods for the determination of the mixing height. Atmos Environm. 34:1001–1027.

Sellers PJ and Dorman JL (1987) Testing the simple biospere model (SiB) for use in general circulation models. J Climate Appl Meteorol. 26:622–651.

Shukauskas A and Schlantschiauskas A (1973) Teploodatscha v turbulentnom potoke shidkosti (Heat exchange in the turbulent fluid). Izd. Mintis, Vil'njus, 327 pp.

Smagorinsky J (1963) General circulation experiments with the primitive equations: I. The basic experiment. Monthly Weather Review. 91:99–164.
Smith SD, Fairall CW, Geernaert GL and Hasse L (1996) Air-sea fluxes: 25 years of progress. Boundary-Layer Meteorol. 78:247–290.
Sodemann H and Foken T (2004) Empirical evaluation of an extended similarity theory for the stably stratified atmospheric surface layer. Quart J Roy Meteorol Soc. 130:2665–2671.
Sponagel H (1980) Zur Bestimmung der realen Evapotranspiration landwirtschaftlicher Kulturpflanzen. Geologisches Jahrbuch. F9:87 pp.
Staudt K, Serafimovich A, Siebicke L, Pyles RD and Falge E (2011) Vertical structure of evapotranspiration at a forest site (a case study). Agrical Forest Meteorol. 151:709–729.
Stull RB (1988) An Introduction to Boundary Layer Meteorology. Kluwer Acad. Publ., Dordrecht, Boston, London, 666 pp.
Stull R and Santoso E (2000) Convective transport theory and counter-difference fluxes. 14th Symposium on Boundary Layer and Turbulence, Aspen, CO., 7.-11. Aug. 2000. Am. Meteorol. Soc., Boston, pp. 112–113.
Sverdrup HU (1937/38) On the evaporation from the ocean. J. Marine Res. 1:3–14.
Taylor PA (1987) Comments and further analysis on the effective roughness length for use in numerical three-dimensional models: A research note. Boundary-Layer Meteorol. 39:403–418.
Tennekes H (1973) A Model for the Dynamics of the Inversion Above a Convective Boundary Layer. J Atmos Sci. 30:558–567.
Troen I and Lundtang Peterson E (1989) European Wind Atlas. Risø National Laboratory, Roskilde, 656 pp.
Turc L (1961) Évaluation des besoins en eau d'irrigation évapotranspiration potentielle. Ann Agron. 12:13–49.
van Bavel CHM (1986) Potential evapotranspiration: The combination concept and its experimental verification. Water Resources Res. 2:455–467.
Vollmer L, van Dooren M, Trabucchi D, Schneemann J, Steinfeld G, Witha B, Trujillo J and Kühn M (2015) First comparison of LES of an offshore wind turbine wake with dual-Doppler lidar measurements in a German offshore wind farm. J Phys: Conf Ser. 625:012001.
von Kármán T (1934) Turbulence and skin friction. J. Aeronautic Sci. 1:1–20.
Wendling U, Schellin H-G and Thomä M (1991) Bereitstellung von täglichen Informationen zum Wasserhaushalt des Bodens für die Zwecke der agrarmeteorologischen Beratung. Z Meteorol. 41:468–475.
Yokoyama O, Gamo M and Yamamoto S (1979) The vertical profiles of the turbulent quantities in the atmospheric boundary layer. J Meteor Soc Japan. 57:264–272.
Zilitinkevich SS and Calanca P (2000) An extended similarity theory for the stably stratified atmospheric surface layer. Quart J Roy Meteorol Soc. 126:1913–1923.
Zilitinkevich SS and Esau IN (2005) Resistance and heat transfer laws for stable and neutral planetary layers: Old theory advanced and re-evaluated. Quart J Roy Meteorol Soc. 131:1863–1892.
Zilitinkevich SS and Mironov DV (1996) A multi-limit formulation for the equilibrium depth of a stable stratified atmospheric surface layer. Boundary-Layer Meteorol. 81:325–351.
Zilitinkevich SS, Perov VL and King JC (2002) Near-surface turbulent fluxes in stable stratification: Calculation techniques for use in general circulation models. Quart J Roy Meteorol Soc. 128:1571–1587.